

# TiO<sub>2</sub>-Based Schottky Diodes as Bidirectional Switches for Bipolar Resistive Memories

Xijian Zhang, Jidong Jin, Jaekyun Kim, Claudio Balocco, Jiawei Zhang, and Aimin Song\*

This study presents TiO<sub>2</sub>-based Schottky diodes designed as bidirectional switches for bipolar resistive memories. The TiO<sub>2</sub> films in these Schottky diodes are prepared through an anodization process. The reverse current of these diodes exhibits an exponential increase with rising reverse voltage, ultimately matching the forward current. When two diodes are connected back-to-back, they demonstrate superior current–voltage symmetry and provide a wider off-state voltage range compared to a single diode, reaching up to 3.65 V. The adjustable off-state voltage range (0.40–3.65 V) of the switch, whether utilizing two diodes or a single diode, correlates well with the TiO<sub>2</sub> layer thickness and oxygen partial pressure during Pt electrode sputtering. These diodes possess bidirectional switching characteristics and can serve as effective switch elements to address the sneak-path issue in bipolar resistive memories.

## 1. Introduction

Resistance random access memory (RRAM), which features a metal–insulator–metal structure that exhibits an electrically-induced resistive switching effect, has gained significant attention for its potential as a next-generation nonvolatile memory.<sup>[1–5]</sup> RRAM combines the advantages of flash and dynamic random access memories while avoiding several drawbacks and demonstrating high scalability potential.<sup>[6]</sup> To achieve high-density storage, RRAM devices can be arranged in a crossbar matrix, with each intersection representing an individual memory cell.<sup>[7]</sup> The cell size can be scaled down to  $4F^2$  (where  $F$  denotes the feature size used

for patterning the cell), which is the smallest cell size attainable in nonvolatile memories with planar structures.<sup>[8]</sup> However, in a crossbar matrix, RRAM faces the sneak-path issue, involving undesired leakage current through the unselected cells.<sup>[1]</sup> To address this issue, a switch element is necessary for each memory cell to control access.<sup>[9,10]</sup>

The 1T1R (one transistor, one resistor) and 1D1R (one diode, one resistor) circuit architectures are commonly employed to reduce sneak paths in RRAM matrices by incorporating additional switch elements (transistor or diode).<sup>[7,11,12]</sup> Although the 1T1R approach significantly reduces crosstalk and signal disturbances within a crossbar matrix, it requires additional space for the transistor contacts, which is unfavorable for achieving high-density integration.<sup>[13]</sup> In the 1D1R configuration, the inclusion of a conventional diode is suitable for unipolar operation in RRAM matrices but unsuitable for bipolar operations, as the reverse current is usually too small to program an RRAM cell, especially during the reset process.<sup>[1]</sup>

Here, we develop Schottky diodes that possess significant bidirectional switching characteristics, making them excellent switch elements for bipolar resistive memories. To attain these bidirectional switching capabilities, we present a novel method for achieving large reverse currents in Pt/TiO<sub>2</sub>/Ti Schottky diodes. This is facilitated by the practical growth of TiO<sub>2</sub> thin films with desired thickness at room temperature through an anodization process. Anodization stands out as one of the most promising thin-film deposition techniques due to its low cost and capacity for large-area deposition.<sup>[14]</sup> By selecting an appropriate TiO<sub>2</sub> thickness, the reverse current of these diodes can match the forward current in magnitude. These diodes exhibit a low-current region at low


X. Zhang, J. Zhang  
Shandong Technology Center of Nanodevices and Integration  
School of Integrated Circuits  
Shandong University  
Jinan 250100, China

J. Jin, J. Kim  
Department of Photonics and Nanoelectronics  
Hanyang University  
Ansan 15588, Republic of Korea

C. Balocco  
Department of Engineering  
Durham University  
Durham DH1 3LE, UK

A. Song  
Institute of Nanoscience and Applications  
Southern University of Science and Technology  
Shenzhen 518055, China  
E-mail: a.song@manchester.ac.uk

A. Song  
Department of Electrical and Electronic Engineering  
University of Manchester  
Manchester M13 9PL, UK

 The ORCID identification number(s) for the author(s) of this article can be found under <https://doi.org/10.1002/pssr.202400156>.

© 2024 The Author(s). physica status solidi (RRL) Rapid Research Letters published by Wiley-VCH GmbH. This is an open access article under the terms of the Creative Commons Attribution License, which permits use, distribution and reproduction in any medium, provided the original work is properly cited.

DOI: 10.1002/pssr.202400156

voltages (indicative of the off-state of a switch) and two high-current regions at high voltages (indicative of the on-state of a switch) making them suitable for use as bidirectional switches in bipolar resistive memories. Furthermore, when two diodes are connected back-to-back, they demonstrate enhanced switch characteristics and current–voltage symmetry compared to a single diode.

## 2. Results and Discussion

**Figure 1a** illustrates the current density–voltage ( $J$ – $V$ ) curves of the Schottky diodes fabricated using 3 and 6 nm  $\text{TiO}_2$  layers, with the Pt electrodes of both diodes deposited using pure Ar. The inset of **Figure 1a** presents a schematic of the fabricated Schottky diodes. These diodes exhibit large reverse currents. The thickness of the semiconductor in Schottky diodes plays a crucial role in determining the magnitude of the reverse current.<sup>[15]</sup> As a general trend, when the semiconductor's thickness decreases, the reverse current increases. Considering the relative thinness of the 3 and 6 nm  $\text{TiO}_2$  layers, electrons can more easily tunnel through the barrier, thus contributing to the observed large reverse current.

The current transport through Schottky diodes can be described by the thermionic emission model:<sup>[16]</sup>

$$J = J_s \left\{ \exp \left[ \frac{q(V - JR_s)}{nkT} \right] - 1 \right\} \quad (1)$$

$$J_s = A^* T^2 \exp \left( \frac{-q\phi_B}{kT} \right) \quad (2)$$

where  $J_s$  is the reverse saturation current density,  $A^*$  is the Richardson constant,  $T$  is the temperature in Kelvin,  $\phi_B$  is the effective barrier height,  $k$  is the Boltzmann constant,  $q$  is the electron charge,  $n$  is the ideality factor, and  $R_s$  is the series resistance.  $A^*$  has a theoretical value of  $1082 \text{ A cm}^{-2} \text{ K}^{-2}$ , calculated from the relation of  $A^* = 4\pi q m^* k^2 / h^3$  by using  $m^* = 9m_e$ .<sup>[17]</sup> Here,  $m^*$  is the electron effective mass,  $h$  is the Planck constant, and  $m_e$  is the free electron mass. By fitting the  $J$ – $V$  curves with Equation (1) and (2),  $\phi_B$  can be extracted.  $R_s$  can be estimated from the linear differential  $dV/dJ$  of  $J$ – $V$  curves at the highest measuring voltage, where the current is mainly limited by the series resistance.<sup>[18]</sup> The fitting results are shown in **Table 1**. The barrier heights of the diodes fabricated with 3 and 6 nm  $\text{TiO}_2$  layers are 0.64 and

**Table 1.** Parameters of the Schottky diodes.

Working gas for sputtering Pt	Anodizing voltage [V]/ Thickness of $\text{TiO}_2$ [nm]	$\phi_B$ [eV]	$R_s$ [ $\Omega$ ]
Pure Ar	2/3	0.64	50
	4/6	0.67	80
95% Ar + 5% $\text{O}_2$	2/3	0.70	6 k
	4/6	1.00	14 k

0.67 eV, respectively. The off-state of the switch is defined as a current density two orders of magnitude lower than the maximum tested current density of the diode. Consequently, diodes with 3 and 6 nm  $\text{TiO}_2$  layers have off-state bias voltage ranges of 0.50 and 0.77 V respectively. **Figure 1b** shows the  $J$ – $V$  curves of the Schottky diodes fabricated using 3 and 6 nm  $\text{TiO}_2$  layers, with the Pt electrodes of both diodes deposited using 95% Ar and 5%  $\text{O}_2$ . Using Equation (1) and (2), the extracted parameters of the diodes are shown in **Table 1**. As shown in **Table 1**, when Pt deposition was conducted with 5%  $\text{O}_2$ , the barrier heights of the Schottky diodes with 3 and 6 nm  $\text{TiO}_2$  layers increased relative to devices with Pt electrodes deposited in pure Ar. This increase in barrier heights may be attributed to the formation of oxidized metal Schottky contacts, which reduces interface defects between the semiconductor and Schottky contacts.<sup>[19–21]</sup> It is important to note that the sputtering of Pt in an  $\text{O}_2/\text{Ar}$  mixture can effectively reduce the number of oxygen vacancies in the oxide semiconductor at the interface.<sup>[21]</sup> This not only leads to the formation of a more ideal and higher Schottky barrier but also a reduced carrier concentration in  $\text{TiO}_2$ . The latter is expected to result in a higher series resistance, consistent with the findings presented in **Table 1**. Another likely reason for a higher series resistance is that the  $\text{O}_2/\text{Ar}$  atmosphere during the Pt sputtering process may further oxidize Ti, resulting in a thicker  $\text{TiO}_2$  layer.

The inset of **Figure 1b** presents the relationship between current density  $J$  and electric field  $E$ , specifically,  $\ln J$  versus  $E^{1/2}$  for both forward and reverse bias conditions. The observed linearity in this curve confirms that the Schottky emissions dominate the transport mechanism under high forward and reverse bias.<sup>[22,23]</sup> As shown in **Figure 1b**, the diode with a 3 nm  $\text{TiO}_2$

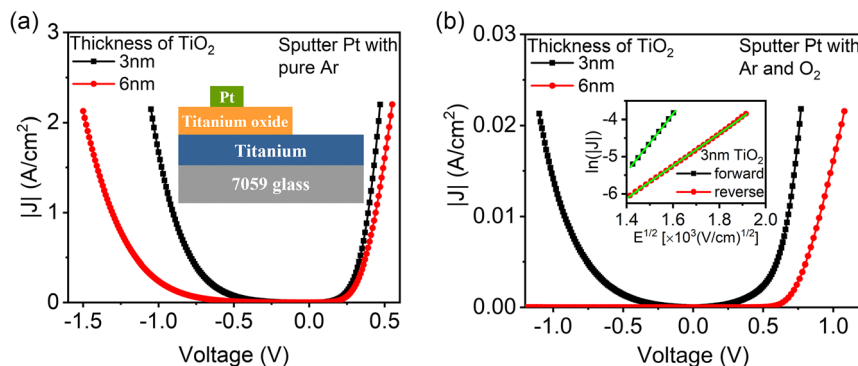


**Figure 1.** Current density as a function of bias voltage ( $J$ – $V$ ) of the  $\text{TiO}_2$  Schottky diodes fabricated with different thicknesses of  $\text{TiO}_2$  layer, Pt electrodes were deposited by sputtering with a) pure Ar or b) 95% Ar and 5%  $\text{O}_2$ . The inset in (a) shows a schematic cross-sectional view of the  $\text{TiO}_2$  Schottky diodes, while the inset in (b) shows the Schottky-emission fitting of  $\ln J$  vs  $E^{1/2}$ .

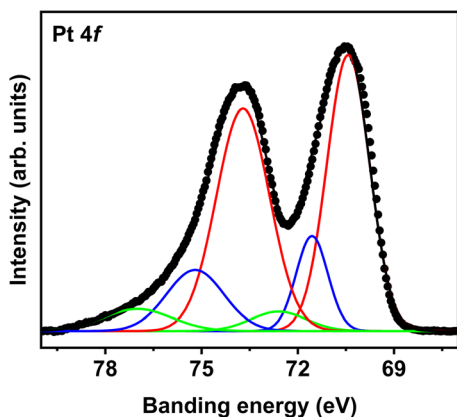


**Figure 2.** Pt 4f core levels of the Pt film deposited by sputtering with 95% Ar and 5% O<sub>2</sub>.

layer demonstrates bidirectional switching capabilities, with a barrier height of 0.7 eV. Conversely, the diode with a 6 nm TiO<sub>2</sub> layer exhibits conventional Schottky diode characteristics. This disparity arises from the increased barrier height, reaching 1 eV, effectively suppressing the reverse current in the latter configuration.

To verify the formation of oxidized Pt Schottky contacts, we conducted X-ray photoelectron spectroscopy (XPS) measurements. **Figure 2** shows the Pt 4f core level of the Pt film deposited by sputtering with 95% Ar and 5% O<sub>2</sub>. The XPS spectrum was deconvoluted into three subpeaks: a pair of peaks (red) at 70.4 and 73.7 eV corresponding to metallic Pt, a pair of peaks (blue) at 71.6 and 75.2 eV corresponding to PtO, and a pair of peaks (green) at 72.6 and 77.0 eV corresponding to Pt(OH)<sub>2</sub>. The XPS measurements confirm that the Pt film deposited by sputtering in the Ar and O<sub>2</sub> mixture is partially oxidized.

To enhance *J*–*V* symmetry and broaden the off-state voltage range for the switch, we implemented a double diode reverse connection mode. This arrangement, depicted in the inset of **Figure 3a**, features two Schottky diodes connected back-to-back. Notably, the left diode is forward biased, while the right diode is reverse biased. This configuration typically results in symmetrical nonohmic behavior in response to both negative and positive bias.<sup>[24,25]</sup> This back-to-back device was fabricated with 3 and

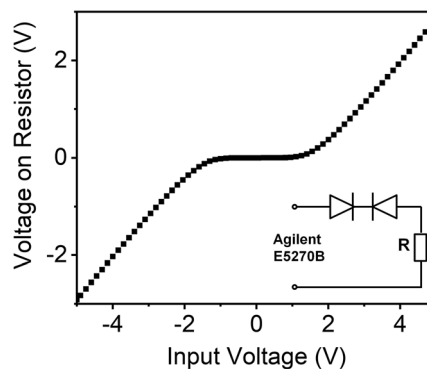


**Figure 4.** Output voltage on the resistor as a function of input voltage. The inset shows the measurement circuit.

6 nm anodized layers of TiO<sub>2</sub> on Ti, with the two Pt electrodes deposited using either pure Ar or a mixture of 95% Ar and 5% O<sub>2</sub>. **Figure 3a** shows the *J*–*V* curves of the device utilizing a double diode reverse connection mode, with the Pt electrodes deposited using pure Ar during the sputtering. The forward and reverse currents exhibit a symmetrical exponential increase, with off-state widths measuring 0.92 V for the 3 nm TiO<sub>2</sub> device and 1.68 V for the 6 nm TiO<sub>2</sub> device. **Figure 3b** shows the *J*–*V* curves of the device utilizing a double diode reverse connection mode, with the Pt electrodes deposited using a mixture of 95% Ar and 5% O<sub>2</sub>. The forward and reverse currents exhibit a symmetrical exponential increase, with off-state widths measuring 2.04 V for the 3 nm TiO<sub>2</sub> device and 3.65 V for the 6 nm TiO<sub>2</sub> device.

A 100 kΩ resistor was connected in series with Schottky diodes utilizing a double diode reverse connection mode, as depicted in the inset of **Figure 4**. These diodes were fabricated using 3 nm TiO<sub>2</sub> layers, and the Pt electrodes were deposited with 95% Ar and 5% O<sub>2</sub>. **Figure 4** displays the voltage across the 100 kΩ resistor as a function of input voltage. The plot reveals an off-state width of 2.04 V, with the majority of the input voltage distributed across the two back-to-back Schottky diodes in the off-state. Consequently, in the off-state, negligible voltage is applied to the resistor, resulting in negligible current flow. This characteristic makes the double diode reverse connection mode well-suited to function as a bidirectional switch for bipolar resistive memory.

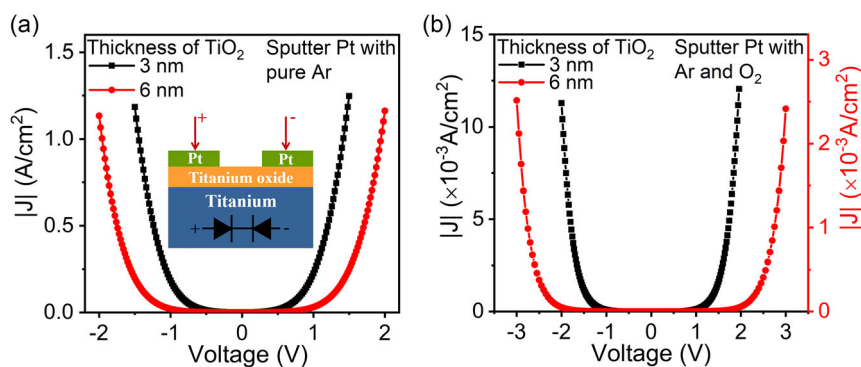


**Figure 3.** Current density as a function of bias voltage (*J*–*V*) of the device in double diode reverse connection mode, Pt electrodes were deposited by sputtering with a) pure Ar or b) 95% Ar and 5% O<sub>2</sub>.

The presented overall footprint of the back-to-back diode configuration is large because it requires two lateral contacts. It is possible to significantly reduce the footprint by constructing a vertical back-to-back architecture. For instance, first deposit Pt as the bottom anode and then Ti. After fully anodizing the Ti layer, deposit another thicker Ti layer, which is then partially anodized to create a second TiO<sub>2</sub> layer with a thickness identical to the first. Finally, deposit the top Pt anode. Such a configuration would enable a footprint compatible with that of the RRAM device, allowing for high memory density.

### 3. Conclusion

In this study, we have introduced TiO<sub>2</sub>-based Schottky diodes designed as bidirectional switches for bipolar resistive memories. These diodes employ TiO<sub>2</sub> films prepared through an anodization process, with thicknesses of 3 and 6 nm, achieved through anodization at 2 and 4 V, respectively. The reverse current of these diodes exhibits an exponential increase as the reverse voltage rises, ultimately aligning with the forward current. Additionally, connecting two diodes back-to-back demonstrated improved current-voltage symmetry and a border off-state voltage range compared to a single diode. The adjustable off-state voltage range (0.40–3.65 V) of the switch, whether utilizing two diodes or a single diode, correlates well with the TiO<sub>2</sub> thickness and oxygen partial pressure during Pt electrode sputtering. These diodes showcase significant bidirectional switching characteristics, positioning them as effective switch elements to address the sneak-path issue in bipolar resistive memories.

### 4. Experimental Section

The Pt/TiO<sub>2</sub>/Ti Schottky diodes, as depicted in the inset of Figure 1a, were fabricated on Corning 7059 glass substrates. First, 100 nm-thick Ti films were deposited onto the glass substrates using RF magnetron sputtering, with an Ar pressure of 1.2 Pa and an RF power of 30 W. Subsequently, the Ti film was anodized at room temperature in 10<sup>-3</sup> M citric acid at 2 and 4 V with a constant current density of 0.1 mA cm<sup>-2</sup> delivered with a Keithley 2400 Source Meter. The anodized TiO<sub>2</sub> layer thicknesses were estimated to be 3 and 6 nm by using an anodization ratio of 1.5 nm V<sup>-1</sup>.<sup>[26]</sup> Additional spectroscopic ellipsometry (J.A. Woollam Co. Inc) was conducted over the wavelength range 200 and 1000 nm at three angles of incidence (65°, 70°, and 75°), which confirmed these thickness estimations. Finally, a circular Pt pad with an area of 1 × 10<sup>-3</sup> cm<sup>2</sup> and a thickness of 50 nm was deposited by RF magnetron sputtering using either pure Ar or a mixed gas (comprising 95% Ar and 5% O<sub>2</sub>), to form the Schottky anode via a shadow mask. Notably, the barrier height of the diode was found to be influenced by the oxygen partial pressure during the sputtering process. During J–V measurements, the top Pt electrode was biased positively and the bottom Ti electrode was grounded.

Schottky diodes utilizing a double diode reverse connection mode, as depicted in the inset of Figure 2a, were fabricated. The fabrication process involved growing 3 and 6 nm TiO<sub>2</sub> layers grown on Ti using the aforementioned anodization method. Subsequently, two Pt electrodes were deposited onto the TiO<sub>2</sub>, employing either pure Ar or a mixture of 95% Ar and 5% O<sub>2</sub> during sputtering. Finally, a 100 kΩ resistor was connected in series with the Schottky diode utilizing a double diode reverse connection mode, where the two Pt electrodes were deposited using pure Ar during sputtering. The voltage across the 100 kΩ resistor was measured as a function of input voltage. The electrical characteristics of the devices were measured using an Agilent E5270B semiconductor analyzer.

### Acknowledgements

X.Z. and J.J. contributed equally to this work. This research was supported by the National Key Research and Development Program of China under grant 2022YFB3603900, the National Natural Science Foundation of China under grant 62074094, the Natural Science Foundation of Shandong Province under grant ZR2022ZD04, and the Korea Basic Science Institute (National Research Facilities and Equipment Center) grant funded by the Ministry of Education under grant 2021R1A6C101A405.

### Conflict of Interest

The authors declare no conflict of interest.

### Data Availability Statement

The data that support the findings of this study are available from the corresponding author upon reasonable request.

### Keywords

bidirectional switches, bipolar resistive memory, Schottky diodes, titanium oxide

Received: April 30, 2024

Revised: June 5, 2024

Published online:

- [1] F. Pan, S. Gao, C. Chen, C. Song, F. Zeng, *Mater. Sci. Eng. R: Rep.* **2014**, *83*, 1.
- [2] J. S. Lee, S. Lee, T. W. Noh, *Appl. Phys. Rev.* **2015**, *2*, 031303.
- [3] M. L. Urquiza, M. M. Islam, A. C. T. van Duin, X. Cartoixà, A. Strachan, *ACS Nano* **2021**, *15*, 12945.
- [4] F. Zahoor, T. Z. Azni Zulkifli, F. A. Khanday, *Nanoscale Res. Lett.* **2020**, *15*, 90.
- [5] G. U. Kamble, A. P. Patil, R. K. Kamat, J. H. Kim, T. D. Dongale, *ACS Appl. Electron. Mater.* **2023**, *5*, 2454.
- [6] R. Waser, M. Aono, *Nat. Mater.* **2007**, *6*, 833.
- [7] Y. Deng, P. Huang, B. Chen, X. Yang, B. Gao, J. Wang, L. Zeng, G. Du, J. Kang, X. Liu, *IEEE Trans. Electron Devices* **2013**, *60*, 719.
- [8] Y. C. Chen, H. Li, W. Zhang, R. E. Pino, *IEEE Trans. Nanotechnol.* **2012**, *11*, 948.
- [9] M. Son, J. Lee, J. Park, J. Shin, G. Choi, S. Jung, W. Lee, S. Kim, S. Park, H. Hwang, *IEEE Electron Device Lett.* **2011**, *32*, 1579.
- [10] M. Wang, W. Wang, W. R. Leow, C. Wan, G. Chen, Y. Zeng, J. Yu, Y. Liu, P. Cai, H. Wang, D. Ielmini, X. Chen, *Adv. Mater.* **2018**, *30*, 1802516.
- [11] M. Zackriya, H. M. Kittur, A. Chin, *Sci. Rep.* **2017**, *7*, 42375.
- [12] T.-W. Kim, H. Choi, S.-H. Oh, G. Wang, D.-Y. Kim, H. Hwang, T. Lee, *Adv. Mater.* **2009**, *21*, 2497.
- [13] R. Waser, R. Dittmann, G. Staikov, K. Szot, *Adv. Mater.* **2009**, *21*, 2632.
- [14] X. Lin, Q. Xin, J. Kim, J. Jin, J. Zhang, A. Song, *IEEE Trans. Electron Devices* **2023**, *70*, 537.
- [15] X. Zhang, W. Cai, J. Zhang, J. Brownless, J. Wilson, Y. Zhang, A. Song, *IEEE Electron Device Lett.* **2019**, *40*, 1378.
- [16] L. Du, J. Zhang, Y. Li, M. Xu, Q. Wang, A. Song, Q. Xin, *IEEE Trans. Electron Devices* **2018**, *65*, 4326.

- [17] C. Kormann, D. W. Bahnemann, M. R. Hoffmann, *J. Phys. Chem.* **1988**, *92*, 5196.
- [18] Q. Xin, L. Yan, L. Du, J. Zhang, Y. Luo, Q. Wang, A. Song, *Thin Solid Films* **2016**, *616*, 569.
- [19] M. W. Allen, R. J. Mendelsberg, R. J. Reeves, S. M. Durbin, *Appl. Phys. Lett.* **2009**, *94*, 103508.
- [20] A. Chasin, S. Steudel, K. Myny, M. Nag, T.-H. Ke, S. Schols, J. Genoe, G. Gielen, P. Heremans, *Appl. Phys. Lett.* **2012**, *101*, 113505.
- [21] T. Schultz, S. Vogt, P. Schlupp, H. von Wenckstern, N. Koch, M. Grundmann, *Phys. Rev. Appl.* **2018**, *9*, 064001.
- [22] H. Altuntas, C. Ozgit-Akgun, I. Donmez, N. Biyikli, *J. Appl. Phys.* **2015**, *117*, 155101.
- [23] S. Kumar, M. V. Kumar, S. Krishnaveni, *Semiconductors* **2020**, *54*, 169.
- [24] A. J. Chiquito, C. A. Amorim, O. M. Berengue, L. S. Araujo, E. P. Bernardo, E. R. Leite, *J. Phys.: Condens. Matter* **2012**, *24*, 225303.
- [25] R. Labar, T. K. Kundu, *J. Electron. Mater.* **2022**, *51*, 223.
- [26] L. A. Majewski, R. Schroeder, M. Grell, *Adv. Mater.* **2005**, *17*, 192.